



[DONATE](#) [HELP](#) [CONTACT AHA](#) [SIGN IN](#) [HOME](#)

Ame

[ADVANCED SEARCH](#)

[Feedback](#) [Subscriptions](#) [Archives](#) [Search](#) [Table of Contents](#)

# Circulation

Receive content via email! **e-toc**

Institution: CLEVELAND HLTH SCI LIBR [Sign In as Member/Individual \(Non-Member\)](#) [Subscription Activation](#)

(*Circulation*. 1996;94:2572-2579.)  
© 1996 American Heart Association, Inc.

*This Article*

- ▶ [Abstract](#) **FREE**
- ▶ [Alert me when this article is cited](#)
- ▶ [Alert me if a correction is posted](#)
- ▶ [Citation Map](#)

*Services*

- ▶ [Email this article to a friend](#)
- ▶ [Similar articles in this journal](#)
- ▶ [Similar articles in PubMed](#)
- ▶ [Alert me to new issues of the journal](#)
- ▶ [Download to citation manager](#)
- ▶ [Cited by other online articles](#)

*PubMed*

- ▶ [PubMed Citation](#)
- ▶ [Articles by Kiehn, J.](#)
- ▶ [Articles by Brown, A. M.](#)

## Articles

### Molecular Physiology and Pharmacology of *HERG*

#### Single-Channel Currents and Block by Dofetilide

Johann Kiehn, MD; Antonio E. Lacerda, PhD; Barbara Wible, PhD; Arthur M. Brown, MD, PhD

the Rammelkamp Center for Research, MetroHealth Campus, Case Western Reserve University, Cleveland, Ohio.

Correspondence to A.M. Brown, Rammelkamp Center, 2500 MetroHealth Dr, Cleveland, OH 44109-1998.

## ▶ Abstract

**Background** The human ether-a-go-go-related gene (*HERG*) is one locus for the hereditary long-QT syndrome. A hypothesis is that *HERG* produces the repolarizing cardiac potassium current  $I_{Kr}$ , with the consequence that mutations in *HERG* prolong the QT interval by reducing  $I_{Kr}$ . The elementary properties of *HERG* are unknown, and as a test of the hypothesis that *HERG* produces  $I_{Kr}$ , we compared their elementary properties.

**Methods and Results** We injected *HERG* cRNA into *Xenopus* oocytes and measured currents from single channels or current variance from the noise produced by ensembles of channels recorded from macro patches. Single-channel conductance was dependent on the extracellular potassium concentration ( $[K]_o$ ). At physiological  $[K]_o$ , it was 2 picosiemens (pS), and at 100

- ▲ [Top](#)
- [Abstract](#)
- ▼ [Introduction](#)
- ▼ [Methods](#)
- ▼ [Results](#)
- ▼ [Discussion](#)
- ▼ [References](#)

mmol/L  $[K]_o$ , it was 10 pS. Openings occurred in bursts with a mean duration of 26 ms at -100 mV. Mean open time was 3.2 ms and closed times were 1.0 and 26 ms. In excised macro patches, *HERG* currents were blocked by the class III antiarrhythmic drug dofetilide, with an  $IC_{50}$  of 35 nmol/L. Dofetilide block was slow and greatly attenuated at positive potentials at which *HERG* rectifies.

**Conclusions** The microscopic physiology of *HERG* and  $I_{Kr}$  is similar, consistent with *HERG* being an important component of  $I_{Kr}$ . The pharmacology is also similar; dofetilide appears to primarily block activated channels and has a much lower affinity for closed and inactivated channels.

**Key Words:** genes • potassium channels • dofetilide • electrophysiology

## ► Introduction

The delayed rectifier  $K^+$  current is responsible for repolarization of the cardiac action potential<sup>1</sup> and can be separated into two components on the basis of kinetic and pharmacological differences.<sup>2 3 4</sup> For the latter,  $I_{Kr}$  is blocked by class III methanesulfonanilides and  $I_{Ks}$  is not. Block of  $I_K$  is clinically

important because class III antiarrhythmic drugs are widely used in the therapy of cardiac arrhythmias. One dramatic side effect is torsade de pointes tachyarrhythmias, frequently in combination with bradycardia and hypokalemia. The pathophysiology of this acquired arrhythmia is unknown, and therefore it is of particular interest to investigate the nature of block on the primary molecular target.

Recently, it has been proposed that  $I_{Kr}$  is encoded by *HERG*, a gene first isolated from a human hippocampal library.<sup>5</sup> Two observations support this idea: First, one form of the hereditary long-QT syndrome (LQT 2) is linked to mutations at the *HERG* locus 7q35-36<sup>6 7</sup>; second, *HERG* expressed heterologously in *Xenopus* oocytes produces whole-cell currents with properties similar to  $I_{Kr}$  in cardiomyocytes.<sup>8</sup> A defective  $I_{Kr}$  readily explains LQT 2.

An initial test of the relationship between *HERG* and  $I_{Kr}$  would be a comparison of their elementary properties. Although the elementary currents of  $I_{Kr}$  have been described, elementary currents of *HERG* are unknown. In the present study, we measured single-channel currents and noise from *HERG* channels expressed heterologously in *Xenopus* oocytes in physiological and high extracellular  $[K]_o$  solutions. We found that the conductance and kinetics of *HERG* currents strongly resemble single-channel  $I_{Kr}$  currents in cardiomyocytes.<sup>9 10</sup> There are strong

▲	<a href="#">Top</a>
▲	<a href="#">Abstract</a>
■	<a href="#">Introduction</a>
▼	<a href="#">Methods</a>
▼	<a href="#">Results</a>
▼	<a href="#">Discussion</a>
▼	<a href="#">References</a>

pharmacological similarities as well. Both *HERG* and  $I_{Kr}$  are blocked by nanomolar concentrations of the class III drug dofetilide. We concluded that *HERG* is a major component of  $I_{Kr}$ .

## ► **Methods**

### **Electrophysiology**

*Xenopus* oocyte measurements were performed by use of the standard two-microelectrode voltage clamp technique.<sup>11</sup> Macro-patch currents were recorded with the use of patch pipettes made from borosilicate glass with tip openings of 10 to 15  $\mu\text{m}$ .<sup>12</sup> After a giga-seal was achieved, patches were excised and positioned in the stream of a large pipette (diameter, 2 mm) to achieve faster solution exchange. Dofetilide was applied to the cytoplasmic surface of the inside-out patches by changing the solution flowing through the application pipette. Single-channel recordings were performed by use of pipettes pulled from hard borosilicate glass with resistances of 2 to 5 M $\Omega$ . Pipettes were coated with Sylgard 184 (Dow Corning) and fire-polished immediately before use.

### **Solutions and Drug Administration**

Two-microelectrode voltage clamp measurements of *Xenopus* oocytes were performed in a low  $\text{K}^+$  solution containing (in mmol/L) 5 KCl, 100 NaCl, 1.5  $\text{CaCl}_2$ , 2  $\text{MgCl}_2$ , and 10 HEPES (pH 7.3). In the measurements with different  $[\text{K}]_o$ , equivalent amounts of NaCl were replaced by KCl.

For macro-patch and single-channel recordings, the 100 mmol/L  $\text{K}^+$  pipette solution contained (in mmol/L) 100 KCl, 2  $\text{MgCl}_2$ , and 10 HEPES (pH 7.3); the 5 mmol/L  $\text{K}^+$  pipette solution contained (in mmol/L) 5 KCl, 100 NaCl, 1.5  $\text{CaCl}_2$ , 2  $\text{MgCl}_2$ , and 10 HEPES (pH 7.3); the 300 mmol/L  $\text{K}^+$  pipette solution contained (in mmol/L) 300 KCl, 1.5  $\text{CaCl}_2$ , 2  $\text{MgCl}_2$ , and 10 HEPES (pH 7.3); and the 50 mmol/L  $\text{K}^+$  pipette solution contained (in mmol/L) 50 KCl, 50 NaCl, 1.5  $\text{CaCl}_2$ , 2  $\text{MgCl}_2$ , and 10 HEPES (pH 7.3). The bath solution in all single-channel and macro-patch measurements contained (in mmol/L) 100 KCl, 1  $\text{MgCl}_2$ , and 10 HEPES (pH 7.3).

Dofetilide (*N*-[4-(-{[4-(methanesulphonamino)phenoxy]-*N*-methylethylamino}ethyl) phenyl] methanesulphonamide; Pfizer Central Research, Sandwich, Kent, England) was dissolved in distilled water, acidified to pH 3.0 by addition of HCl to make a 10-mmol/L stock solution, and stored at  $-20^\circ\text{C}$ . On the day of experiments, aliquots of the stock solution were diluted to the desired concentration. All measurements were made at room temperature ( $20^\circ\text{C}$ ).

### **Data Analysis**

Data were low-pass filtered at 1 to 2 kHz (-3 dB, four-pole Bessel filter) before digitalization at 5 to 10 kHz. PClamp software (Axon Instruments) was used for generation of the voltage-pulse

▲	<a href="#">Top</a>
▲	<a href="#">Abstract</a>
▲	<a href="#">Introduction</a>
▪	<a href="#">Methods</a>
▼	<a href="#">Results</a>
▼	<a href="#">Discussion</a>
▼	<a href="#">References</a>

protocols and for data acquisition. All single-channel measurements were analyzed by use of Transit software.<sup>13</sup> This resulted in histograms for amplitudes, open times, closed times, and burst duration. Probability density function parameter estimates were obtained with the maximum likelihood method and gave values for  $\tau_{\text{open}}$ ,  $\tau_{\text{closed1}}$ ,  $\tau_{\text{closed2}}$ , and  $\tau_{\text{burst}}$ .

For nonstationary noise analysis, data were collected in 30 traces of 2000 sample points, resulting in 60 000 points for noise power spectrum frequency evaluation. Data were analyzed by use of the Fourier transform. Analysis was accomplished with the Solver add-in to Microsoft Excel 7.0 and Windows NT 3.51. Spectral density analysis of *HERG* unitary current fluctuations was performed with Mathematica 2.2.3. The power spectrum [S(f)] was fitted with a sum of two Lorentzian functions<sup>14</sup>:  $S(f) = S_1(0)/[1+(f/f_{c1})^2] + S_2(0)/[1+(f/f_{c2})^2]$ , where  $S_1(0)$  and  $S_2(0)$  are the low-frequency intercepts and  $f_{c1}$  and  $f_{c2}$  are the corner frequencies. The fitting routine was as follows: First, the noise spectrum was fitted with a single Lorentzian function to obtain  $f_{c1}$  and  $S_1(0)$ . These values were inserted and held constant in the double Lorentzian equation to obtain  $f_{c2}$  and  $S_2(0)$ . Estimates of power and  $f_{c2}$  from the high-frequency component,  $S_2(f)$ , were judged too variable for further study because of its small magnitude relative to background noise. From the best-fit  $f_c$  values, we calculated the relaxation time constant ( $\tau_1$ ), which is an expression of channel kinetics, according to the following equation:  $\tau = 1/(2\pi f_c)$ .

Currents were fitted by a single exponential equation,  $I = I_{\text{max}} \exp[-(t-t_0)/\tau_{\text{on}}] + C$ , where  $I_{\text{max}}$  is the maximum current during the test pulse,  $t_0$  is the start time of the test pulse, and  $\tau_{\text{on}}$  is the time constant of blocking. C is a constant, ie, an incomplete block by dofetilide during the test pulse.

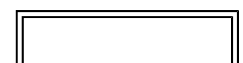
The measured  $IC_{50}$  values were used to calculate the half-maximal blocking concentration by fitting a dose-response curve to the normalized current values ( $I_{\text{drug}}/I_{\text{control}}$ ). The normalized current was expressed as a function of the dofetilide concentration according to the following binding equation:  $I_{\text{drug}}/I_{\text{control}} = 1/(1+X/IC_{50})^n$ , where X is the dofetilide concentration and n is the Hill coefficient. Statistical data are presented as mean $\pm$ SD.

### Molecular Biology

The *HERG* clone was a gift from M.T. Keating.<sup>6</sup> The pSP64 construct containing *HERG* was linearized with *EcoRI* (Boehringer Mannheim) and transcribed into cRNA with the mMACHINE mMACHINE in vitro transcription kit (Ambion) by use of SP6 polymerase.

RNA (50 to 500 ng/ $\mu$ L) was injected into *Xenopus* oocytes, and measurements were made 2 to 8 days after injection.

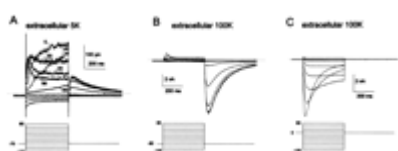
## ► Results



## Macroscopic Currents

In cell-attached macro patches, we made measurements at different extracellular  $[K]_o$  concentrations. At a physiological  $[K]_o$  of 5 mmol/L, *HERG* showed current kinetics that resemble  $I_{Kr}$ .<sup>3 15 16</sup> From a holding potential of -70 mV, the current activated at potentials of -40 mV or above. At 20, 40, and 60 mV, the steady-state currents became progressively smaller (inward rectification) (Fig 1A\*) and were preceded by transient peaks. These transient peaks were observed in all patches and recordings from whole oocytes. During the step back to -70 mV, outward deactivating tail currents were preceded by an initial rising phase due to fast recovery from inactivation.<sup>8 17</sup>

▲ [Top](#)  
 ▲ [Abstract](#)  
 ▲ [Introduction](#)  
 ▲ [Methods](#)  
 ■ [Results](#)  
 ▼ [Discussion](#)  
 ▼ [References](#)



**View larger version (15K):**  
[\[in this window\]](#)  
[\[in a new window\]](#)

**Figure 1.** Macro-patch currents of *HERG* expressed in *Xenopus* oocytes. A, Holding potential: -70 mV; test pulse: -120 to 60 mV in 20-mV steps (400 ms); return pulse: -70 mV (400 ms). Bath: 100 mmol/L  $K^+$ ; pipette: 5 mmol/L  $K^+$ . B, Holding potential: -80 mV; test pulse: -120 to 60 mV in 20-mV steps (400 ms); return pulse: -80 mV (400 ms). Bath: 100 mmol/L  $K^+$ ; pipette: 100 mmol/L  $K^+$ . C, Holding potential: 0 mV; test pulse: -120 to 60 mV in 20-mV steps (400 ms); return pulse: 0 mV (400 ms). Bath: 100 mmol/L  $K^+$ ; pipette: 100 mmol/L  $K^+$ .

At 100 mmol/L  $[K]_o$ , the outward currents rectified inwardly and had transient peaks at 20, 40, and 60 mV (Fig 1B\*) that inactivated more slowly than at 5 mmol/L  $[K]_o$ . During steps back to -80 mV, large inward tail currents were evoked (Fig 1\*B). When the same protocol with a holding potential of 0 mV was used, only large inward tail currents were observed. Because of inactivation at 0 mV, the outward currents at 20, 40, and 60 mV were much smaller (Fig 1C\*). In both measurements, a rising phase or "hook" in the tail currents due to recovery from inactivation preceded deactivation (Fig 1B and 1C\*\*). Fig 1C\* demonstrates that the rates of recovery are voltage dependent, with faster recovery occurring at more negative potentials. Tail current deactivation was also voltage dependent; at -20 and -40 mV, there was virtually no deactivation, and from -60 to -120 mV, the deactivation rate increased with hyperpolarization (Fig 1C\*).

The kinetics of the macro-patch currents were identical to whole-oocyte measurements under the same conditions (data not shown).<sup>18</sup> When macro patches were excised into a solution containing 0  $Mg^{2+}$  for 10 minutes, the current kinetics did not change (n=5 patches; data not shown).

## Single-Channel Currents

In 100 mmol/L  $[K]_o$ , we measured single-channel currents at hyperpolarized potentials in both cell-attached and inside-out configurations. From a holding potential of -80 mV, channels were

activated by a prepulse to 0 mV for 1 second before a hyperpolarizing step to -120 mV. In excised patches, the openings had a mean amplitude of 1.1 pA (Fig 2\*). Openings were more frequent at the beginning of the steps to -120 mV and occurred in bursts. The average of 32 traces with at least four channels had the same time course as the macroscopic tail currents at -120 mV (Fig 2\*). The hook (recovery from inactivation) is apparent in the averaged trace (Fig 2\*). Subsequent deactivation was fitted with a single exponential function that had a  $\tau$  of 87 ms, which is identical to the macro-patch tail current  $\tau$  of  $89 \pm 25$  ms ( $n=6$ ) (Fig 1C\*, lowest trace). At 5 mmol/L  $[K]_o$ , single-channel currents were not observed.

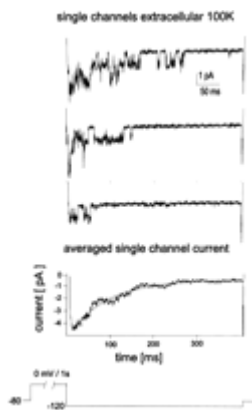
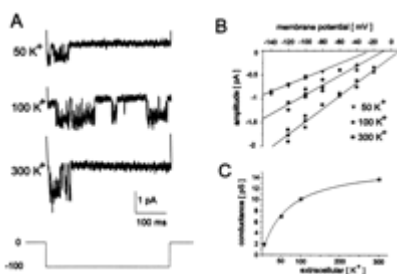


**Figure 2.** Single-channel recordings of *HERG* expressed in *Xenopus* oocytes. The averaged trace of 32 measurements with at least four channels in the patch mimics the time course of the macro-patch current at -120 mV (compare with Fig 1C\*) with 100 mmol/L extracellular  $K^+$ . Holding potential: -80 mV; prepulse: 0 mV (1000 ms); test pulse: -120 mV (400 ms). Bath: 100 mmol/L  $K^+$ ; pipette: 100 mmol/L  $K^+$ .

**View larger version**  
(20K):  
[\[in this window\]](#)  
[\[in a new window\]](#)

We measured single-channel currents at different  $[K]_o$  in excised patches (Fig 3A\*). From a holding potential of -80 mV, channels were activated by a prepulse to 0 mV/1 second, and single-channel currents were measured by hyperpolarizing to -100 mV. The amplitude of the single-channel currents depended strongly on  $[K]_o$ . At -100 mV, single-channel currents were  $0.55 \pm 0.02$  ( $n=2$ ),  $0.89 \pm 0.06$  ( $n=4$ ), and  $1.47 \pm 0.12$  pA ( $n=3$ ) in 50, 100, and 300 mmol/L  $[K]_o$ , respectively.



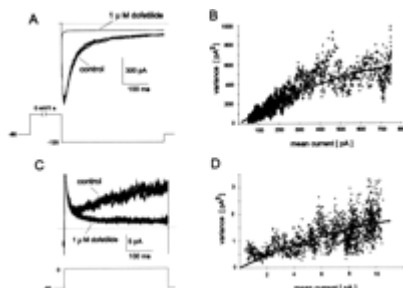
**View larger version** (22K):  
[\[in this window\]](#)

**Figure 3.** A, Single-channel measurements at different extracellular potassium concentrations: Holding potential: -80 mV; prepulse: 0 mV (1000 ms); test pulse: -100 mV (400 ms). Bath: 100 mmol/L  $K^+$ ; pipette: 100 mmol/L  $K^+$ . B, Graphic display of multiple measurements at different extracellular  $K^+$  concentrations. Straight lines are linear fits to measured values. C, Graphic display of the calculated single-channel conductance versus extracellular  $K^+$

[\[in a new window\]](#)

concentration. The conductance ( $S$ ) versus  $[K]_o$  was fitted by a Michaelis-Menten curve according to the following equation<sup>19</sup>:  $S([K]_o) = S_{max} / \{1 + (K_{1/2} / [K]_o)\}$ , where  $S_{max}$  is the saturating conductance and  $K_{1/2}$  is the potassium concentration at half-maximal conductance. The extracellular  $K^+$  concentration for half-maximal conductance was 64 mmol/L.

In Fig 3B\*, single-channel currents are plotted as functions of membrane potential at different  $[K]_o$ . We calculated slope conductances by fitting straight lines to the measured values. The single-channel conductance was 7.0, 10.1, and 13.7 pS with 50, 100, and 300 mmol/L  $[K]_o$ , respectively. The conductance is displayed as a function of extracellular potassium concentration in Fig 3C\*. The value at 5 mmol/L  $K^+$  was obtained from nonstationary noise analysis (Fig 5\*). To these data, we fitted a Michaelis-Menten function<sup>19</sup> (Fig 3C\*). The half-maximal conductance was reached at 64 mmol/L  $[K]_o$  and the conductance saturates at 16.6 pS.



**View larger version (28K):**

[\[in this window\]](#)

[\[in a new window\]](#)

**Figure 5.** Variance measurements to calculate the single-channel conductance: A, Control measurement and block of the current with 1  $\mu$ mol/L dofetilide in 100 mmol/L extracellular  $K^+$  (5 traces are displayed). B, Variance analysis of 48 traces and the corresponding nonlinear least-squares fit of variance against the mean current indicated a single-channel amplitude of 1.21 pA. C, Control measurement and block of the current with 1  $\mu$ mol/L dofetilide in 5 mmol/L extracellular  $K^+$  (5 traces are displayed). D, Variance analysis of 36 traces shows a single-channel amplitude of 0.23 pA at 5 mmol/L extracellular  $K^+$ . A and B: Holding potential: -80 mV; prepulse: 0 mV (1000 ms); test pulse: -120 mV (400 ms). Bath: 100 mmol/L  $K^+$ ; pipette: 100 mmol/L  $K^+$ . C and D: Holding potential: -80 mV; test pulse: 0 mV (400 ms). Bath: 100 mmol/L  $K^+$ ; pipette: 5 mmol/L  $K^+$ .

At -100 mV in symmetrical 100 mmol/L  $K^+$  ( $n=3$ ), the amplitude distribution had a peak at  $0.86 \pm 0.11$  pA (Fig 4A\*). The open-time distribution was a monoexponential function with  $\tau_{open} = 3.2 \pm 1.2$  ms (Fig 4B\*). Channel closed-time distributions were biexponential, with  $\tau_{closed1} = 1.0 \text{ ms} \pm 0.4 \text{ ms}$  and  $\tau_{closed2} = 22.3 \pm 3.5$  ms (Fig 4C\*). The burst-duration distribution was monoexponential, with  $\tau_{burst} = 25.9 \pm 5.93$  ms (Fig 4D\*).

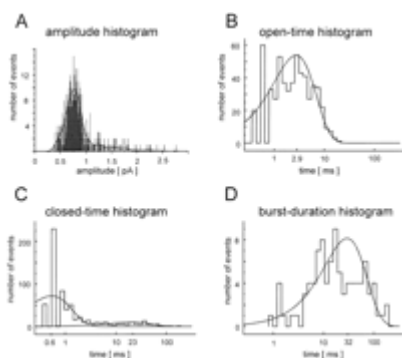


**Figure 4.** Single-channel kinetic parameters of *HERG* in a typical inside-out patch. Analysis was performed with 32 traces and 590 openings at -100 mV membrane potential. A, Single-channel amplitude histogram shows a peak at 0.76 pA. B, The open-time distribution shows an open time of 2.9 ms. C, Closed-time distribution was fitted with two closed times (0.6 and 23 ms). D, Burst-duration distribution was 32 ms.

View larger version (29K):

[\[in this window\]](#)

[\[in a new window\]](#)

### Nonstationary Noise Currents at Physiological $[K]_o$

Single-channel conductance decreased as extracellular  $[K]_o$  was lowered (Fig 3 $\blacklozenge$ ). In 5 mmol/L  $[K]_o$ , single-channel currents could not be resolved. However, macro-patch currents became obviously noisy at activating potentials (Fig 1A $\blacklozenge$ ). Therefore, we performed nonstationary noise analysis on these currents. We first established the validity of our method with 100 mmol/L  $[K]_o$ , at which concentration single-channel currents were resolved. We measured 16 to 48 noise traces, then blocked the current completely with 1  $\mu$ mol/L dofetilide to obtain background capacitive and leak currents (Fig 5A $\blacklozenge$ ). The mean of the blocked traces was then subtracted from each noise trace. The single-channel amplitude ( $i$ ) was calculated, according to  $\sigma^2 = iI - I^2/N$ ,<sup>20 21</sup> where  $\sigma^2$  is the variance of the currents,  $I$  is the mean current, and  $N$  is the number of channels. At 100 mmol/L  $[K]_o$ , the single-channel current was calculated to be  $0.9 \pm 0.2$  pA ( $n=2$ ) and the conductance was 9 pS (Fig 5B $\blacklozenge$ ), values virtually identical to those for resolved openings under the same conditions (Fig 3 $\blacklozenge$ ).

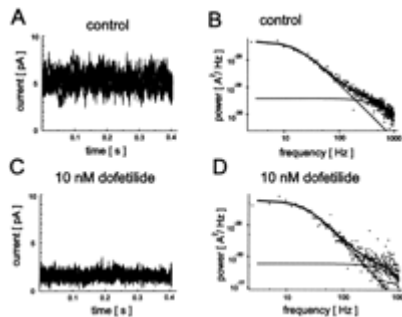
At 5 mmol/L  $[K]_o$  and 0 mV, we calculated a single-channel current of  $0.2 \pm 0.1$  pA ( $n=3$ ) and a single-channel conductance of 2 pS.

### Block of Microscopic Currents by Dofetilide

When patches were excised into a solution containing 100 nmol/L dofetilide, single-channel activity decreased within 2 to 3 minutes during repetitive pulsing at a frequency of 0.2 Hz. We analyzed single-channel currents and found no significant changes in amplitude ( $i$ ), open time, closed times, and burst duration compared with control (Fig 4 $\blacklozenge$ ). In 100 nmol/L dofetilide, the single-channel parameters were  $i=0.79 \pm 0.13$  pA,  $\tau_{open}=4.5 \pm 2.9$  ms,  $\tau_{closed1}=0.85 \pm 0.2$  ms,  $\tau_{closed2}=25.8 \pm 5.5$  ms, and  $\tau_{burst}=27.1 \pm 4.5$  ms ( $n=3$ ).

To extend our analysis to more physiological  $[K]_o$ , we analyzed the power spectral density of macro-patch steady-state currents at 0 mV in 5 mmol/L  $[K]_o$ . The  $\tau$  of the fits to the data is an

expression of channel kinetics and was  $\tau_1=8.06\pm 1.36$  ms ( $f_{c1}=20.06\pm 3.13$  Hz) for control (n=3). When dofetilide at 10 nmol/L was applied for 10 minutes to an inside-out macro patch, the noise magnitude was greatly reduced. The  $\tau$  was slightly reduced to  $\tau_1=5.9\pm 1.15$  ms ( $f_{c1}=27.2\pm 5.14$  Hz) (Fig 6C $\blacktriangleright$ ). Washout of the dofetilide block was extremely slow. In two patches (patches D5630 and A5630), noise frequency was partially restored after 10 to 20 minutes ( $\tau_1=7.5\pm 0.42$  ms;  $f_{c1}=21.15\pm 1.2$  Hz).

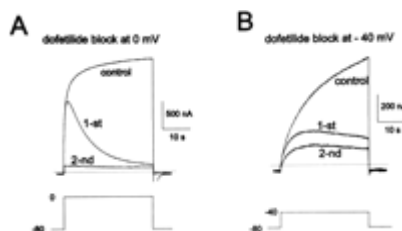


View larger version (29K):  
[\[in this window\]](#)  
[\[in a new window\]](#)

**Figure 6.** Steady-state macro-patch currents in a typical inside-out macro patch in the absence (A) and presence (C) of 10 nmol/L dofetilide (five traces each are displayed). Note that the current amplitude and noise were reduced by dofetilide. B and D show the corresponding noise frequency spectra with a double Lorentzian fit (thick line) and both of its components (thin lines). The corner frequencies for the control measurements were  $f_{c1}=16.6$  Hz ( $\tau_1=9.6$  ms) and  $f_{c2}=532$  Hz ( $\tau_2=0.22$  ms). The measurements with 10 nmol/L dofetilide gave slightly faster values ( $f_{c1}=22.5$  Hz [ $\tau_1=7.1$  ms] and  $f_{c2}=2142$  Hz [ $\tau_2=0.074$  ms]).

### Block of Macroscopic Currents by Dofetilide

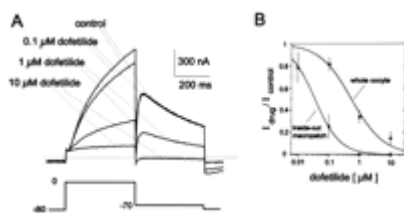
We measured whole-oocyte currents using very long test pulses (32 seconds) to resolve the kinetics of dofetilide block (Fig 7A $\blacktriangleright$ ). After control currents were measured, the membrane potential was held at -80 mV and dofetilide (10  $\mu$ mol/L) was perfused into the bath for 10 minutes. The first test pulse from a holding potential of -80 to 0 mV showed the onset of block (Fig 7 $\blacktriangleright$ ). Repetitive pulsing increased the block in a cumulative manner (first and second pulses in Fig 7A and 7B $\blacktriangleright\blacktriangleright$ ). The block was related to the extent of activation. At -40 mV, the control trace showed a slow time-dependent increase in current during the entire 32-second test pulse. At this potential, block was slower and smaller than at 0 mV.



View larger version (14K):  
[\[in this window\]](#)  
[\[in a new window\]](#)

**Figure 7.** Slow kinetics of dofetilide (10  $\mu$ mol/L) block in double electrode measurements. A, Control measurement and block by dofetilide at 0 mV in the first and second test pulses after wash-in of dofetilide and holding the cell for 10 minutes at -80 mV. B, Control and dofetilide block at -40 mV. Holding potential: -80 mV; test pulse: 0 (A) or -40 mV (B) (32 seconds). Bath: 5 mmol/L K<sup>+</sup>.

To measure the steady-state  $IC_{50}$  values for dofetilide block, we stimulated at a frequency of 1 Hz from a holding potential of -80 mV with a test pulse of 0 mV/400 ms to mimic frequency and duration of the cardiac action potential. At each minute, currents were measured by use of a depolarizing test pulse to 0 mV/400 ms followed by a return pulse to -70 mV/400 ms to record tail currents. Each concentration of dofetilide was washed in for 20 minutes during continuous pulsing. After 10 to 15 minutes, dofetilide block reached steady state. Fig 8A $\blacklozenge$  displays the control trace and the steady-state effects of 0.1, 1, and 10  $\mu\text{mol/L}$  dofetilide, respectively. Fig 8B $\blacklozenge$  displays the fitted dose-response curve at 5 mmol/L  $[K]_o$ . We measured dose-response curves to the end of the 0-mV activating test pulse at different  $[K]_o$  and found that the  $IC_{50}$  was independent of  $[K]_o$  in the range of 2 to 20 mmol/L ( $n=4$  at each  $[K]_o$ ). A similar result was recently obtained with a dofetilide analog, MK-499.<sup>22</sup> Our calculated  $IC_{50}$  values in whole oocytes were 644 nmol/L at 2 mmol/L  $[K]_o$ , 595 nmol/L at 5 mmol/L  $[K]_o$ , and 692 nmol/L at 20 mmol/L  $[K]_o$ .



**View larger version** (19K):  
[\[in this window\]](#)  
[\[in a new window\]](#)

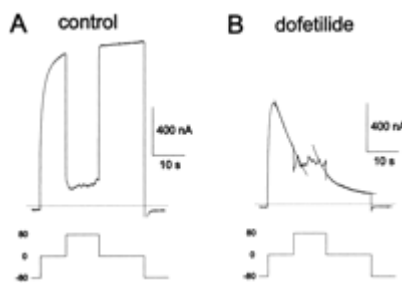
**Figure 8.** A, Concentration dependence of steady-state dofetilide block in whole-oocyte measurements by use of a pulsing protocol. Holding potential: -80 mV, stimulation frequency 1 Hz (0 mV/400 ms); every 60 seconds, one measurement was made. Test pulse: 0 mV (400 ms); return pulse: -70 mV (400 ms); bath: 5 mmol/L  $K^+$ . B, A dose-response curve fitted to the normalized steady-state block currents at the end of 400-ms test pulses gave an  $IC_{50}$  of 595 nmol/L in whole-oocyte measurements ( $n=4$ ) and an  $IC_{50}$  of 35 nmol/L in inside-out macro patches ( $n=6$ ).

Because the  $IC_{50}$ s in whole oocytes were large owing to oocyte yolk and the diffusion barrier of the vitelline membrane, we determined the  $IC_{50}$  for dofetilide in inside-out macro patches in 5 mmol/L  $[K]_o$ . We calculated an  $IC_{50}$  of 35 nmol/L ( $n=6$ ) at the end of a 400-ms/0-mV test pulse using a continuous pulsing protocol analogous to the whole-oocyte measurements (Fig 8B $\blacklozenge$ ). Thus, the  $IC_{50}$  for *HERG* in the cell membrane is similar to values reported for  $I_{Kr}$ .<sup>23</sup>

### Inward Rectification Prevents Block by Dofetilide

To determine whether dofetilide blocked inactivated (rectified) channels, we took advantage of the strong rectification of *HERG* at membrane potentials of  $\geq 20$  mV (Fig 1A $\blacklozenge$ ). We designed a modified protocol with an intervening step to 80 mV to determine how much block occurred when the current rectified strongly compared with a continuous pulse to 0 mV without rectification (Fig 9A $\blacklozenge$ ). The control trace without dofetilide showed the inward rectification during the step at 80 mV (Fig 9A $\blacklozenge$ ). At 80 mV, we observed small current fluctuations that were probably due to activation of endogenous oocyte channels or transporters (Fig 9A $\blacklozenge$ ). Because the

fluctuations were relatively small in amplitude, they were neglected in the analysis. During the step back to 0 mV, the current continued its normal time course (Fig 9A\*).



**View larger version (14K):**  
[\[in this window\]](#)  
[\[in a new window\]](#)

**Figure 9.** Rectification of the *HERG* current prevents block by dofetilide. A, Control measurement with an intervening step to 80 mV in the middle of the measurement. B, Effect of dofetilide (10  $\mu\text{mol/L}$ ). The currents at the 0-mV steps before and after the 80-mV intervening step were fitted monoexponentially, and fits were drawn into the graph. Note the gap of 6.1 seconds between the fitted lines, which resulted from less block during the 80-mV step of the measurement. Holding potential: -80 mV. Test pulse with three steps: step 1, 0 mV (10 seconds); step 2, 80 mV (10 seconds); step 3, 0 mV (12 seconds). Bath: 5 mmol/L  $\text{K}^+$ .

After holding the cell at -80 mV, we added dofetilide and waited for 10 minutes to reach equilibrium. In the first voltage step, the normal kinetics of block at 0 mV by dofetilide were seen (Fig 9B\*). The second step at 80 mV showed current fluctuations similar to control. In the third step at 0 mV, the normal kinetics of dofetilide block were resumed, but the current amplitude in the beginning of this third step was larger than it would have been during a continuous 0-mV step (compare Figs 7A and 9B\*\*). Fits to the currents before and after the intervening step show a discontinuity in the block equivalent to a gap of  $4.9 \pm 1.0$  seconds ( $n=3$ ). We concluded that inward rectification prevented block by dofetilide.

## ► Discussion

### Microscopic Properties of *HERG* and $I_{\text{Kr}}$

*HERG* has a single-channel conductance of 2 pS under physiological conditions. The conductance is dependent on  $[\text{K}]_o$  and saturates at high concentrations. The concentration dependence of the conductance has also been reported for other  $\text{K}^+$  channel clones that have been expressed heterologously.<sup>24</sup> It is consistent with multi-ion occupancy of the ion conduction pathway as occurs in delayed rectifier  $\text{K}^+$  channels.<sup>19</sup>

Our results demonstrate that *HERG* has similar elementary properties to  $I_{\text{Kr}}$ . In symmetrical (100 mmol/L)  $\text{K}^+$  concentrations, we measured a single-channel conductance ( $G$ ) of 10.1 pS, a mean open time of 3.2 ms, and two closed times with time constants of 1.0 and 23 ms.  $I_{\text{K}}$  ( $I_{\text{Kr}}$ ) in sinoatrial nodal cells of the rabbit heart (150 mmol/L  $\text{K}^+$ ) has  $G=11.1$  pS,  $\tau_{\text{open}}=2.5$  ms,  $\tau_{\text{closed1}}=0.7$  ms,  $\tau_{\text{closed2}}=17.6$  ms<sup>17</sup>;  $I_{\text{K}}$  in atrial cardiomyocytes from guinea pig (150 mmol/L

▲	<a href="#">Top</a>
▲	<a href="#">Abstract</a>
▲	<a href="#">Introduction</a>
▲	<a href="#">Methods</a>
▲	<a href="#">Results</a>
■	<a href="#">Discussion</a>
▼	<a href="#">References</a>

$K^+$ ) has  $G=10$  pS,  $\tau_{\text{open}}=9$  ms,  $\tau_{\text{closed1}}=1.2$  ms,  $\tau_{\text{closed2}}=37$  ms<sup>2</sup>;  $I_{K_r}$  in rabbit ventricular cells (150 mmol/L  $K^+$ ) has  $G=13.1$  pS<sup>9</sup>; and  $I_{K_r}$  in human ventricular cardiomyocytes (140 mmol/L  $K^+$ ),  $G=14$  pS.<sup>10</sup> The similarity of unitary conductance and kinetics is strong evidence that *HERG* is a major component of  $I_{K_r}$ . This conclusion is important because  $I_{K_r}$  in human atrium<sup>25</sup> and ventricle<sup>26</sup> is the primary target for class III antiarrhythmic drugs such as dofetilide. Block of  $I_{K_r}$  by class III antiarrhythmic drugs can induce the same type of arrhythmia, torsade de pointes, as that seen in patients with LQT 2, in which the *HERG* gene is mutated.<sup>6</sup>

A difference between *HERG* expressed in *Xenopus oocytes* and  $I_{K_r}$  in cardiomyocytes may lie in the kinetics of the transient peak at positive potentials. A transient peak of  $I_{K_r}$  is clearly observed in human atrial cardiomyocytes<sup>25</sup> (measured as the E-4031-sensitive current) and ferret atrial myocytes,<sup>27</sup> but in our recordings, the peak appeared to be more pronounced, with a faster relaxation.

The prominent tail currents of *HERG* are characteristic and are also observed in  $I_{K_r}$ .<sup>3 15 16</sup> The large amplitudes of the tail currents result from the unusual kinetics of *HERG*. During activating pulses, the majority of channels accumulate rapidly in inactivated states. In the return pulses, the large number of previously inactivated channels recover from inactivation and produce the rising phase (hook) in the tail current. In fact, the tail current amplitude may be even larger than the current amplitude during the activating pulse, although the driving force ( $E_{\text{clamp}}-E_K$ , where  $E_{\text{clamp}}$  is the membrane potential maintained by the voltage clamp amplifier and  $E_K$  is potassium equilibrium potential) is smaller.

### Dofetilide Block

Block of *HERG* by dofetilide has no effect on single-channel conductance. In addition, single-channel current kinetics were not significantly affected during test pulses of several hundred milliseconds. These results indicate that block, especially unblocking, is very slow. Thus, 60 minutes was required to wash out 70% of dofetilide block in the whole oocytes and 10 to 20 minutes in excised patches.

It appears that dofetilide blocks activated *HERG* channels with low affinity to closed and inactivated states for the following reasons. First, the channel is not significantly blocked before activation, because the initial depolarizing pulse to 0 mV (after holding for 10 minutes at -80 mV in the presence of drug) reached a peak amplitude of  $\approx 75\%$  (Fig 7A $\clubsuit$ ). Second, block is prevented when the current rectifies at very positive potentials (Fig 9 $\clubsuit$ ), consistent with low affinity binding of dofetilide to inactivated states of *HERG*. At potentials at which *HERG* rectifies, there are fewer channels in activated states, which results in lessened block.

At present, we cannot determine whether dofetilide blocks the open state, an adjacent activated closed state, or a combination of both, because block is extremely slow. Under our experimental

conditions, dofetilide produced no significant change in channel open time, and different extracellular  $K^+$  concentrations resulted in no significant change in the  $IC_{50}$ . Our spectral density measurements, however, showed a small reversible change in the low-frequency component. The recorded spectral densities were dominated by fast transitions into and out of the open state, and the low sensitivity of these to dofetilide is consistent with the observed lack of effect on single-channel gating parameters. The observed increase in  $f_{c1}$  (and reduction of  $\tau_1$ ) may be the result of dofetilide reduction of channel open time or burst duration or a combination of both. Termination of bursts or clusters of bursts by dofetilide binding to an activated closed state would be consistent with our experimental data.

Recently, it has been reported<sup>28</sup> that block of  $I_{Kr}$  in AT1 tumor cells by dofetilide is  $[K]_o$  dependent with weaker block at high  $[K]_o$ . The reason for this difference versus our measurements with  $[K]_o$ -independent block of *HERG* is unknown.<sup>22</sup>

It is likely that dofetilide acts intracellularly, because the onset of block in excised macro patches was faster (2 minutes) than in whole-oocyte measurements, for which it took  $\approx 10$  minutes to reach steady-state block. At physiological pH, dofetilide is 28.5% protonated and positively charged.<sup>29</sup> We suspect that the drug diffuses through the oocyte membrane to reach its point of action intracellularly. This idea is further supported by whole-cell measurements in isolated guinea pig cardiomyocytes, in which, in a rapid perfusion system, a time delay of 3 minutes was measured from application of the drug to the steady-state block of  $I_{Kr}$ .<sup>16</sup>

The  $IC_{50}$  for block of *HERG* current in inside-out macro patches was 35 nmol/L. This value is similar to dofetilide block of  $I_{Kr}$  in guinea pig cardiomyocytes ( $IC_{50}=30$  nmol/L).<sup>23</sup> The washout of dofetilide in *HERG* is very slow, and slow recovery from block has also been reported for dofetilide in rabbit cardiomyocytes.<sup>30</sup> Thus, dofetilide block of *HERG* expressed in *Xenopus* oocytes and  $I_{Kr}$  in cardiomyocytes is similar.

*HERG* is not the only molecular target for dofetilide. Recently, we demonstrated<sup>31 32</sup> that hIRK, a cloned inward rectifier  $K^+$  channel from human atrium, is blocked by dofetilide with an  $IC_{50}$  of 530 nmol/L at 40 mV in inside-out patches in the absence of the physiological blockers  $Mg^{2+}$  and polyamines.<sup>33 34 35</sup> Block of hIRK by dofetilide is very different, however. It is an open-channel block that is reduced at higher  $[K]_o$  and has a fast on rate (hIRK:  $k_{on}=3.1 \times 10^6$  mol/L<sup>-1</sup>·s<sup>-1</sup> at 100 mV).<sup>32 36</sup>

To summarize, we have shown that *HERG* expressed heterologously in *Xenopus* oocytes has similar biophysical and pharmacological properties to  $I_{Kr}$  measured in guinea pig, rabbit, and human cardiomyocytes. Separation of  $I_{Kr}$  from other  $K^+$  currents is difficult and requires drug block and subtraction. Also, human cardiomyocytes are not generally available for the study of

$I_{K_r}$ . A practical consequence of our experiments is that heterologous expression of *HERG* in *Xenopus* oocytes is a useful method to study  $I_{K_r}$  and  $I_{K_r}$  blockers in human heart.

## ▶ Selected Abbreviations and Acronyms

$I_K$	= delayed rectifier potassium current
$I_{K_r}$	= rapid component of the delayed rectifier potassium current
$I_{K_s}$	= slow component of the delayed rectifier potassium current
$[K]_o$	= extracellular potassium concentration
LQT 2	= one form of the hereditary long-QT syndrome
pA	= picoampere
pS	= picosiemen
$\tau$	= relaxation time constant

## ▶ Acknowledgments

Dr Kiehn was supported by a grant of the Deutsche Forschungsgemeinschaft, and Dr Brown was supported by NIH grants HL-55404 and HL-36930. We thank P. Kiehn and Dr W.Q. Dong for technical assistance, Dr M. Keating for providing the *HERG* clone, and Drs E. Ficker and Z. Wang for helpful discussions.

Received March 13, 1996; revision received June 25, 1996; accepted July 5, 1996.

## ▶ References

1. Carmeliet E. Mechanisms and control of repolarization. *Eur Heart J.* 1993;14(suppl H):3-13.
2. Horie M, Hayashi S, Kawai C. Two types of delayed rectifying  $K^+$  channels in atrial cells of guinea pig heart. *Jpn J Physiol.* 1990;40:479-490. [[Medline](#)]
3. Sanguinetti MC, Jurkiewicz NK. Two components of cardiac delayed rectifier  $K^+$  current. *J Gen Physiol.* 1990;96:195-215. [[Abstract](#)]

▲ <a href="#">Top</a>
▲ <a href="#">Abstract</a>
▲ <a href="#">Introduction</a>
▲ <a href="#">Methods</a>
▲ <a href="#">Results</a>
▲ <a href="#">Discussion</a>
▪ <a href="#">References</a>

4. Chinn K. Two delayed rectifiers in guinea pig ventricular myocytes distinguished by tail current kinetics. *J Pharmacol Exp Ther.* 1993;264:553-560.[\[Abstract\]](#)
5. Warmke J, Ganetzky B. A family of potassium channel genes related to *EAG* in *Drosophila* and mammals. *Proc Natl Acad Sci U S A.* 1994;91:3438-3442.[\[Abstract\]](#)
6. Curran ME, Splawski I, Timothy KW, Vincent GM, Green ED, Keating MT. A molecular basis for cardiac arrhythmia: *HERG* mutations cause long QT syndrome. *Cell.* 1995;80:795-804.[\[Medline\]](#)
7. Keating MT. Genetic approaches to cardiovascular disease: supravulvular aortic stenosis, Williams syndrome, and long-QT syndrome. *Circulation.* 1995;92:142-147.[\[Abstract/Free Full Text\]](#)
8. Sanguinetti MC, Jiang C, Curran ME, Keating MT. A mechanistic link between an inherited and an acquired cardiac arrhythmia: *HERG* encodes the  $I_{Kr}$  potassium channel. *Cell.* 1995;81:1-8.[\[Medline\]](#)
9. Veldkamp MW, van Ginneken ACG, Bouman LN. Single delayed rectifier channels in the membrane of rabbit ventricular myocytes. *Circ Res.* 1993;72:865-878.[\[Abstract\]](#)
10. Veldkamp MW, van Ginneken AC, Opthof T, Bouman LN. Delayed rectifier channels in human ventricular myocytes. *Circulation.* 1995;92:3497-3504.[\[Abstract/Free Full Text\]](#)
11. Taglialatela M, Wible BA, Caporaso R, Brown AM. Specification of pore properties by the carboxyl terminus of inward rectifier  $K^+$  channels. *Science.* 1994;264:844-847.[\[Medline\]](#)
12. Hilgemann DW, Nicoll DA, Philipson KD. Charge movement during  $Na^+$  translocation by native and cloned cardiac  $Na^+/Ca^+$  exchanger. *Nature.* 1991;352:715-718.[\[Medline\]](#)
13. VanDongen AMJ. A new algorithm for idealizing single ion channel data containing multiple unknown conductance levels. *Biophys J.* 1996;70:1303-1315.[\[Abstract\]](#)
14. Neher E, Stevens CF. Conductance fluctuations and ionic pores in membranes. *Annu Rev Biophys Bioeng.* 1977;6:345-381.[\[Medline\]](#)
15. Yang R, Snyders DJ, Roden DM. Ibutilide, a methanesulfonanilide antiarrhythmic, is a potent blocker of the rapidly activating delayed rectifier  $K^+$  current ( $I_{Kr}$ ) in AT-1 cells. *Circulation.* 1995;91:1799-1806.[\[Abstract/Free Full Text\]](#)
16. Kiehn J, Villena P, Beyer T, Brachmann J. Differential effects of the new class III agent dofetilide on potassium currents in guinea pig cardiomyocytes. *J Cardiovasc Pharmacol.* 1994;24:566-572.[\[Medline\]](#)
17. Shibasaki T. Conductance and kinetics of delayed rectifier potassium channels in nodal cells of the rabbit heart. *J Physiol.* 1987;387:227-250.[\[Abstract\]](#)
18. Trudeau MC, Warmke JW, Ganetzky B, Robertson GA. HERG, a human inward rectifier

- in the voltage gated potassium channel family. *Science*. 1995;269:92-95.[\[Medline\]](#)
19. Hille B. *Ionic Channels in Excitable Membranes*. 2nd ed. Sunderland, Mass: Sinauer; 1992.
  20. Sigworth FJ. The variance of current fluctuations at the node of Ranvier. *J Physiol (Lond)*. 1980;307:97-129.[\[Medline\]](#)
  21. Silberberg SD, Magleby KL. Preventing errors when estimating single channel properties from the analysis of current fluctuations. *Biophys J*. 1993;65:1570-1584.[\[Abstract\]](#)
  22. Spector PS, Curran ME, Keating MT, Sanguinetti MC. Class III antiarrhythmic drugs block HERG, a human cardiac delayed rectifier K<sup>+</sup> channel. *Circ Res*. 1996;78:499-503.  
[\[Abstract/Free Full Text\]](#)
  23. Jurkiewicz NK, Sanguinetti MC. Rate-dependent prolongation of cardiac action potential by a methanesulfonanilide class III antiarrhythmic agent: specific block of rapid activating delayed rectifier K<sup>+</sup> current by dofetilide. *Circ Res*. 1993;72:75-83.[\[Abstract\]](#)
  24. Heginbotham L, MacKinnon R. Conduction properties of the cloned shaker K<sup>+</sup> channel. *Biophys J*. 1993;65:2089-2096.[\[Abstract\]](#)
  25. Wang J, Fermini B, Nattel S. Rapid and slow components of delayed rectifier current in human atrial myocytes. *Cardiovasc Res*. 1994;28:1540-1546.[\[Medline\]](#)
  26. Li GR, Feng JL, Yue LX, Carrier M, Nattel S. Evidence for two components of delayed rectifier K<sup>+</sup> current in human ventricular myocytes. *Circ Res*. 1996;78:689-696.  
[\[Abstract/Free Full Text\]](#)
  27. Liu S, Rasmusson RL, Campbell DL, Wang S, Strauss HC. Activation and inactivation kinetics of an E-4031-sensitive current from single ferret atrial myocytes. *Biophys J*. 1996;70:2704-2715.[\[Abstract\]](#)
  28. Yang T, Roden DM. Extracellular potassium modulation of drug block by I<sub>Kr</sub>. *Circulation*. 1996;93:407-411.[\[Abstract/Free Full Text\]](#)
  29. Cross PE, Arrowsmith JE, Thomas GN, Gwilt M, Burges A, Higgins AJ. Selective class III antiarrhythmic agents: 1 Bis(arylalkyl)amines. *J Med Chem*. 1990;33:1151-1155.[\[Medline\]](#)
  30. Carmeliet E. Voltage- and time-dependent block of the delayed K<sup>+</sup> current in cardiac myocytes by dofetilide. *J Pharmacol Exp Ther*. 1992;262:809-817.[\[Abstract\]](#)
  31. Wible BA, DeBiasi M, Majumder K, Tagliatela M, Brown AM. Cloning and functional expression of an inwardly rectifying K<sup>+</sup> channel from human atrium. *Circ Res*. 1995;76:343-350.[\[Abstract/Free Full Text\]](#)
  32. Kiehn J, Wible B, Ficker E, Tagliatela M, Brown AM. Cloned human inward rectifier potassium channel as a target for class III methanesulfonanilides. *Circ Res*. 1995;77:1151-

1155.[\[Abstract/Free Full Text\]](#)

33. Ficker E, Taglialatela M, Wible BA, Henley CM, Brown AM. Spermine and spermidine as gating molecules for inward rectifier K<sup>+</sup> channels. *Science*. 1994;266:1068-1072.[\[Medline\]](#)
34. Lopatin AN, Makhina EN, Nichols CG. Potassium channel block by cytoplasmic polyamines as the mechanism of intrinsic rectification. *Nature*. 1994;372:366-369.[\[Medline\]](#)
35. Fakler B, Brandle U, Bond C, Glowatzki E, Koenig C, Adelman JP, Zenner H-P, Ruppersberg JP. A structural determinant of differential sensitivity of cloned inward rectifier K<sup>+</sup> channels to intracellular spermine. *FEBS Lett*. 1994;356:199-203.[\[Medline\]](#)
36. Kiehn J, Wible B, Lacerda A, Brown AM. Mapping the block of a cloned human inward rectifier potassium channel by dofetilide. *Mol Pharmacol*. 1996;50:380-387.[\[Abstract\]](#)